

## FUZZY LOGIC-BASED CHATTERING REDUCTION IN SLIDING MODE CONTROL OF SINGLE-LINK ROBOT USING MUSCLE-LIKE ACTUATOR

MOHAMMED KHAZAAL HAMZAH<sup>1</sup>, RAAED SADOON AL-AZZAWI<sup>1</sup>  
AMMAR AL-JODAH<sup>2</sup>, AMJAD JALEEL HUMAIDI<sup>1</sup> AND ALAQ FALAH HASAN<sup>3</sup>

<sup>1</sup>Control and Systems Engineering Department  
University of Technology  
Al-Sina'a Street, Baghdad 10066, Iraq  
{ 60115; raaed.s.alazzawi; amjad.j.humaidi }@uotechnology.edu.iq

<sup>2</sup>School of Physics, Maths and Computing  
University of Western Australia  
Perth, WA 6907, Australia  
ammr.al-jodah@uwa.edu.au

<sup>3</sup>Technical Engineering College  
Middle Technical University  
Muasker Al Rashid Street, Baghdad 10066, Iraq  
alaaqf.hasan@mtu.edu.iq

Received March 2023; accepted June 2023

**ABSTRACT.** *This paper introduces the concept of fuzzy logic to reduce the chattering effect accompanied by Sliding Mode Control (SMC) in control of single-link robot using muscle-like actuator. In sliding mode control design, the main source of chattering comes from the use of Signum function in the switching part of control signal. This inherited behavior of chattering would degrade the performance of the control systems and may lead to unwanted physical phenomena. To elevate the effect of chattering, many works replaced the discontinuous Signum functions by other different smooth functions. In the present work, Fuzzy Logic (FL) method has been designed and applied in SMC scheme for controlling single-link manipulator actuated by Pneumatic Artificial Muscles (PAMs). The effectiveness of the proposed technique is verified and compared to other switching techniques in terms of performance and chattering reduction via computer simulation. The numerical simulation showed that the chattering has been considerably reduced based on FL-based SMC as compared to Signum-based SMC.*

**Keywords:** Fuzzy logic, Sliding mode control, Chattering phenomenon, Stability analysis

**1. Introduction.** One of the well-known robust method which is robust for the external disturbances and model uncertainties is the Sliding Mode Control (SMC). In this technique, the control system is designed in a way that the states are driven and forced them toward the sliding surface, or even close enough to its neighbor of the switch surface as well. Hence, the closed-loop dynamics are completely governed by the equations that define the surface and all states' trajectories stay within the surface. Thus, the sliding surface is an attractive. However, the reaching phase for such surface usually uses a famous discontinuous function, namely "Signum function", as a switching function. The function works to keep the system trajectories on the sliding surface until they reach their corresponding equilibrium points. In spite of important role of this control function, it has an adverse effect on the performance of actuator, as it causes chattering behavior in the actuating signal and it may excite neglected high-frequency dynamics in the system.

These unwanted chattering behaviors could cause possible damages to the actuators. Nevertheless, in some applications, the chattering is an inevitable behavior for discontinuous switching input systems to maintain some specified performance characteristics for control of these systems [1,2].

Many methodologies are proposed to lessen such chattering; one of them is that, usually, introducing a boundary layer is around the sliding surface. However, such a constraining of the boundary layer costs increased tracking error. In [3,4], the remedy of these drawbacks, both tracking errors and chattering are reduced by adjusting both linear control and the bandwidth of sliding surface layer. However, adjustment is based on tracking error variance. It has been well-known and reported by related researches, there are two famous methodologies, which are responsible for chattering reduction of discontinuous input signals in slide mode control applications [3,4]; one is the boundary layer saturation method, and the second method is based on artificial intelligence.

Although, the first method, boundary layer saturation method, can solve effectively the chattering phenomenon, it has mainly two shortcomings, signified by the increase of error and the reduction in speed of transient response.

In the literature of sliding mode design in different control applications, many researchers have addressed the chattering reduction in control signals. Back to [5], Slotine and Li solved the chattering problem based on linear boundary layer method to enhance the performance of SMC in industrial applications. While in [6], Yang et al. have developed an adaptive fuzzy system as replacing the switching term of the SMC, which is used in control of islanded inverter for power supply system. In [7], Tseng and Chen proposed to use a low-pass filter on the control signal. Such design technique is suitable and outperforms with application of SMC in noisy environments. In [8] a comparison study has been made by Sahamijoo et al. In this study, three methods are adapted chattering reduction purpose of sliding mode control for 3D joint robotic system. These methods are boundary layer method, intelligent method and PD-parallel method. The results of the study show the more suitability of two approaches, parallel PD control and intelligent fuzzy PD controller, than boundary layer approach in terms of chattering attenuation in such three dimensions joint application. In [9], Cibiraj and Varatharajan proposed an Adaptive Neural Gain Scheduling Sliding Mode Control (ANGS-SMC) method for solving the chattering problem. The proposed method ANGS-SMC showed a better reduction result in high frequency components than its rival of Adaptive Fuzzy Gain-Scheduling SMC (AFGS-SMC). A Super-Twisting SMC (STSMC) approach is applied to controlling 2 degree-of-freedom helicopter dynamics [10], by Humaidi and Hasan. The gotten results showed that STSMC can maintain the distinctive robustness features of SMC design; besides that it is successfully providing a smoother control signal than that is gotten via conventional SMC design approach. Unlike [9], Yang and Yan in their research [11] proposed Fuzzy Logic System (FLS) to attenuate the chattering due to Signum function. The FLS is utilized for designing of AFGS-SMC approach to regulate the attitude of unmanned quad-rotors. The idea behind this approach is that control gains are adaptively scheduled according to an appropriate fuzzy rules, with two inputs for the FLS: sliding surface and its derivate of the sliding surface, while control signal gains are represented as FLS outputs.

The motivation behind this study is to use the characteristics of membership functions in fuzzy logic structure instead of using different shapes of switching functions. In this study, the fuzzy logic approach has been introduced in the design of SMC to reduce the chattering behavior in control signal which is used to actuate the PAM-based robot link. The main contributions of this work can be listed as follows.

- 1) Design SMC based on fuzzy logic system to chattering eliminating in the actuating signal in controlling the single-link robot motorized by muscle-like actuator.

- 2) A stability analysis is conducted for the controlled robot based on SMC.
- 3) Conduct a comparison study between the FL-based SMC and Signum-based SMC for controlling the PAM-based robot.

The remainder of the article has been organized in five sections. The dynamic model has been presented in Section 2. The SMC-based design is developed in Section 3, while Section 4 is devoted to the proposed chattering-reduction scheme. The numerical results are shown and discussed in Section 5. The concluded points have been highlighted in Section 6.

**2. The Mathematical Equation of the Manipulator Dynamics.** This section is devoted to developing dynamical equations model for single-link robot arm which is stimulated by PAMs in opposing bicep/tricep passion. The behavior of PAM actuator is similar to real behavior of physical system. After that, the system is analyzed and its associated designed controller meets performance's requirements. The schematic diagram for the robot-model is shown in Figure 1 [12-16].

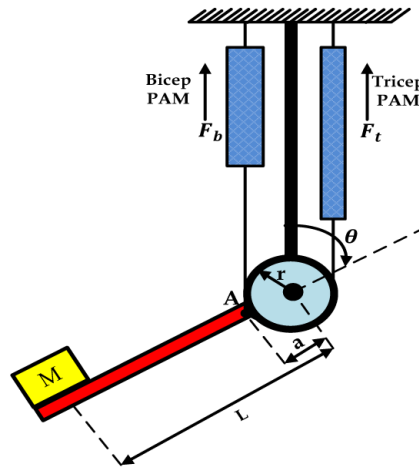


FIGURE 1. The single-link robotic PAM arm [12]

In Figure 1,  $M$  denotes the mass (kg),  $g$  represents the gravitational-acceleration ( $\text{m/s}^2$ ),  $L$  represents the arm length starting from the mass center to the joint-center,  $a$  is the distance from the joint rotation axis to the PM attached point, i.e., (A), and  $r$  represents radius of pulley.

The forearm forms an angle  $\alpha = \arcsin(r/a)$  with tricep cable. The forearm is freely allowed to rotate within this angle range only. As shown in Figure 1 above, the pose of the robot when angle  $\theta = 0$  corresponds to the case that the forearm is in downward pose, while the maximum angle allowable value, i.e.,  $\theta = \pi$ , represents the pose such that the forearm is in extreme upward position [12]. The dynamical motion equation which is derived for the single arm manipulator via Figure 1 is defined as [17-23]

$$\begin{aligned}
 I\ddot{\theta} = & n(F(P_b) - K(P_b)x_b - B_b(P_b)\dot{x}_b) a \sin \theta \\
 & - n(F(P_t) - K(P_t)x_t - B_t(P_t)\dot{x}_t) r - MgL \sin \theta
 \end{aligned} \quad (1)$$

where  $I = ML^2$  denotes the moment of mass inertia about the robot-elbow,  $F(P_t)$  represents the force exerted by PAM in tricep case,  $F(P_b)$  is the force exerted by PAM in bicep case,  $B(P_b)$  represents the bicep coefficient of viscous friction,  $B(P_t)$  represents the tricep coefficient of the viscous friction, while  $K(P_b)$  represents the bicep spring coefficient,  $K(P_t)$  represents the tricep spring coefficient (N/m) and  $n$  is the PAMs' number. It is evident that coefficient  $B$  depends on in what the muscle is posed; in other words, it is either deflated pose or inflated pose. However, one can easily differentiate between

them as follows: The tricep coefficient denotes by  $B(P_t)$  and bicep coefficient denotes by  $B(P_b)$ .

Let  $n = 1$ , and assume coefficients  $F$ ,  $K$  and  $B$  for either bicep/tricep are pressure-dependent functions and, thus, they can be expressed in following Equations (2)-(4):

$$F(P) = F_0 + F_1P \tag{2}$$

$$K(P) = K_0 + K_1P \tag{3}$$

$$B(P) = B_0 + B_1P \tag{4}$$

where  $F_i$ ,  $K_i$  and  $B_i$  for  $i = 0, 1$  represent the coefficients that characterize the functions  $F(P)$ ,  $K(P)$  and  $B(P)$ , respectively. The tricep displacement and bicep displacement  $x_t$ ,  $x_b$  are defined, respectively, by [12]

$$x_b = a(1 - \cos \theta) \tag{5}$$

$$x_t = a(1 + \cos \theta) \tag{6}$$

The first-time-derivatives of  $x_t$  and  $x_b$  are as follows:

$$\dot{x}_b = a \sin \theta \cdot \dot{\theta} \tag{7}$$

$$\dot{x}_t = -a \sin \theta \cdot \dot{\theta} \tag{8}$$

Substituting Equations (5)-(8), into Equation (1), yields

$$I\ddot{\theta} = (F(P_b) - K(P_b)x_b - (B_{0b} + B_{1b}P_b)\dot{x}_b) a \sin \theta - (F(P_t) - K(P_t)x_t - (B_{0t} + B_{1t}P_t)\dot{x}_t) r - MgL \sin \theta \tag{9}$$

Substituting Equations (2)-(4) into Equation (9), yields

$$I\ddot{\theta} = \left( F(P_b) - K(P_b)x_b - a(B_{0b} + B_{1b}P_b) \sin \theta \cdot \dot{\theta} \right) a \sin \theta - \left( F(P_t) - K(P_t)x_t + a(B_{0t} + B_{1t}P_t) \sin \theta \cdot \dot{\theta} \right) r - MgL \sin \theta \tag{10}$$

The tricep and bicep pressures of PAM are given via Equations (11) and (12), shown in the following.

$$P_t = P_{0t} - \Delta P \tag{11}$$

$$P_b = P_{0b} + \Delta P \tag{12}$$

where  $P_{0t}$ ,  $P_{0b}$  are the initial pressure values of the tricep/bicep pressures, respectively, and  $\Delta P$  is the variation of pressure amount. Substituting Equation (11) and Equation (12) into Equation (10), yields

$$I\ddot{\theta} = \left[ (F_0 + F_1P_{0b}) + F_1\Delta P - a(K_0 + K_1P_{0b})(1 - \cos \theta) - aK_1(1 - \cos \theta)\Delta P - a(B_{0b} + B_{1b}P_{0b}) \sin \theta \cdot \dot{\theta} - aB_{1b} \sin \theta \cdot \dot{\theta}\Delta P \right] a \cdot \sin \theta - \left[ (F_0 + F_1P_{0t}) - F_1\Delta P - a(K_0 + K_1P_{0t})(1 + \cos \theta) + aK_1(1 + \cos \theta)\Delta P + a(B_{0t} + B_{1t}P_{0t}) \sin \theta \cdot \dot{\theta} - aB_{1t} \sin \theta \cdot \dot{\theta}\Delta P \right] r - MgL \sin \theta \tag{13}$$

Re-arrange Equation (13) to put it in its compact form:

$$\ddot{\theta} = f(\theta, \dot{\theta}) + b(\theta, \dot{\theta}) \Delta P \tag{14}$$

Let  $u = \Delta P$ , and then Equation (14) becomes

$$\ddot{\theta} = f_o + \Delta f + bu \tag{15}$$

where  $\Delta f$  and  $f_o$  represent the uncertainties and nominal value of  $f(\theta, \dot{\theta})$ , respectively.

The state function  $f_o(\theta, \dot{\theta})$  can be described by

$$f_o(\theta, \dot{\theta}) = \sum_{i=1}^6 f_i Z_i(\theta, \dot{\theta})$$

$$b(\theta, \dot{\theta}) = \sum_{i=1}^6 b_i Z_i(\theta, \dot{\theta})$$

where  $i \in \mathbb{Z}$  and  $i \in [1, 6]$ . The definitions of the elements of the coefficients  $f_i$ ,  $Z_i$  and  $b_i$ , are listed in Table 1.

TABLE 1. Definitions of the elements of the coefficients  $f_i$ ,  $Z_i$  and  $b_i$

$Z_i$	$f_i$	$b_i$
$z_1 = \sin \theta$	$f_1 = (aF_0 + aF_1P_{0b} - MgL)/I$	$b_1 = aF_1/I$
$z_2 = \sin \theta(\cos \theta - 1)$	$f_2 = a^2(K_0 + K_1P_{0b})/I$	$b_2 = a^2K_1/I$
$z_3 = \sin^2 \theta \cdot \dot{\theta}$	$f_3 = -a^2(B_{0b} + B_{1b}P_{0b})/I$	$b_3 = -a^2B_{1b}/I$
$z_4 = 1 + \cos \theta$	$f_4 = ar(K_0 + K_1P_{0t})/I$	$b_4 = -arK_1/I$
$z_5 = \sin \theta \cdot \dot{\theta}$	$f_5 = -ar(B_{0t} + B_{1t}P_{0t})/I$	$b_5 = arB_{1t}/I$
$z_6 = 1$	$f_6 = (-rF_0 - rF_1P_{0t})/I$	$b_6 = rF_1/I$

Equation (15) has its space state variable representation as shown in Equation (16):

$$x_1 = \theta$$

$$\dot{x}_1 = \dot{\theta} = x_2 \tag{16}$$

$$\dot{x}_2 = \ddot{\theta} = \ddot{x}_1 = f_o(x_1, x_2) + b(x_1, x_2)u + \Delta f$$

In Table 2, all the elements of the coefficients definitions are listed for  $f_i$ ,  $Z_i$  and  $b_i$ .

TABLE 2. Definitions of the elements of coefficients  $f_i$ ,  $Z_i$  and  $b_i$  with state space representation

$Z_i$	$f_i$	$b_i$
$z_1 = \sin x_1$	$f_1 = (aF_0 + aF_1P_{0b} - MgL)/I$	$b_1 = aF_1/I$
$z_2 = \sin x_1(\cos x_1 - 1)$	$f_2 = a^2(K_0 + K_1P_{0b})/I$	$b_2 = a^2K_1/I$
$z_3 = \sin^2 x_1 \cdot x_2$	$f_3 = -a^2(B_{0b} + B_{1b}P_{0b})/I$	$b_3 = -a^2B_{1b}/I$
$z_4 = 1 + \cos x_1$	$f_4 = ar(K_0 + K_1P_{0t})/I$	$b_4 = -arK_1/I$
$z_5 = \sin \theta \cdot x_2$	$f_5 = -ar(B_{0t} + B_{1t}P_{0t})/I$	$b_5 = arB_{1t}/I$
$z_6 = 1$	$f_6 = (-rF_0 - rF_1P_{0t})/I$	$b_6 = rF_1/I$

**3. Design of SMC for PAM-Actuated Single-Link Manipulator.** The error  $e = q - q_d$  refers to the difference between the actual and desired angle, respectively. It can be expressed as Equation (17):

$$e = \theta - \theta_d \tag{17}$$

The first-, and second-time-derivatives of the error equation can be gotten through Equations (18) and (19), in respective order:

$$\dot{e} = \dot{\theta} - \dot{\theta}_d \tag{18}$$

$$\ddot{e} = \ddot{\theta} - \ddot{\theta}_d \tag{19}$$

The well-known sliding surface definition, [24-32], as

$$s = \dot{e} + \lambda e \tag{20}$$

For the first time-derivative of the sliding surface  $s$ , Equation (20), the following equation is gotten:

$$\dot{s} = \ddot{\theta} - \ddot{\theta}_d + \lambda \dot{e} \tag{21}$$

Use Equation (16) and Equation (21) to have

$$\dot{s} = f_o - \ddot{\theta}_d + \lambda \dot{e} + \Delta f + bu \tag{22}$$

The control law is made up of two main parts, namely the equivalent part  $u_{eq}$  and the switching part  $u_s$ .

$$u = (1/b)(u_{eq} + u_s) \tag{23}$$

According to Equation (22), the equivalent control law can be deduced by setting  $\dot{s}$  to zero, that is,

$$u_{eq} = -f_o + \ddot{\theta}_d - \lambda \dot{e} \tag{24}$$

Using Equation (23) and Equation (24), Equation (22) becomes

$$\dot{s} = \Delta f + u_s \tag{25}$$

Defining the switching control part as  $u_s = -k \text{sign}(s)$ , Equation (25) becomes [24]

$$\dot{s} = \Delta f - k \text{sign}(s) \tag{26}$$

In order to guarantee the convergence of system trajectories, the reaching condition  $\dot{s}s \leq 0$  has to be satisfied. Then, one can obtain

$$\dot{s}s = s\Delta f - k s \text{sign}(s) \tag{27}$$

or,

$$\dot{s}s = s\Delta f - k|s| \leq |s||\Delta f| - k|s| \leq -|s|(k - |\Delta f|) \tag{28}$$

According to above equation, the reaching condition can be satisfied if the following inequality holds, that is,

$$k > |\Delta f| \tag{29}$$

Thus, according to Equation (29), choice of gain  $k$  must be chosen such that the uncertainties of the system are cancelled. Generally speaking, as higher values of  $k$  are chosen, the higher levels of chattering in the control signal. However, the value  $k = 1$  is chosen as suitable choice in the design of SMC for this application.

**4. Proposed Chattering-Free FL Scheme.** In the proposed FL-based SMC scheme, the control law will be defined by the following equation:

$$u = (1/b)(u_{eq} + u_{sfl}) \tag{30}$$

Instead of using  $u_s$  as Signum function, the switching part is the output of the fuzzy logic system as indicated in Figure 2.

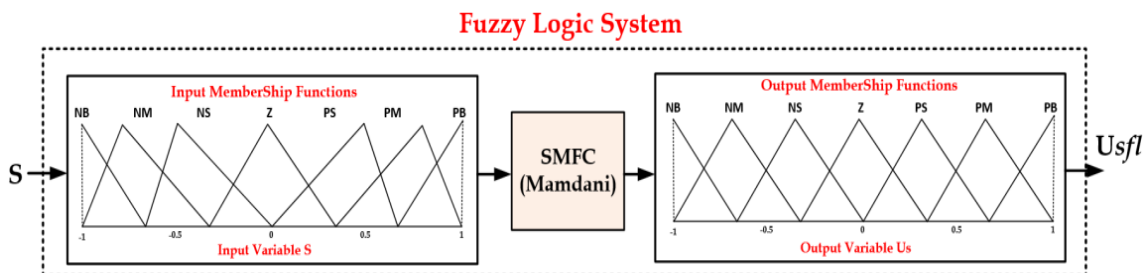


FIGURE 2. The switching part of control law based on FL system

The sliding variable described by Equation (20) is passed through the input Membership Function (MF) of non-symmetric triangular set. Then, set of linguistic rules is synthesized according to Table 3.

TABLE 3. The rule base of the proposed FL system

Knowledge base of FL system		
	IF [ $S =$ ]	THEN [ $U_s =$ ]
1.	NB	NB
2.	NM	NM
3.	NS	NS
4.	Z	Z
5.	PS	PS
6.	PM	PM
7.	PB	PB

In this fuzzy scheme, the mamdani method is used to perform the fuzzy inference. In the defuzzification step, the fuzzy output is converted to crisp value  $u_{sfL}$  by using equi-spaced MFs as described by Figure 2. In this study, the centroid of area has been used to extract the crisp output  $u_{sfL}$ . In this FL system, five MFs have been used for both the input and the output. These MFs represent the linguistic values as the following representations: Z (Zero), NS (Negative Small), NM (Negative Medium), NB (Negative Big), and for positive values, PS (Positive Small), PM (Positive Medium), and PB (Positive Big) [33-38].

**5. Numerical Simulation.** The single-link manipulator is powered by pneumatic muscles (tricep and bicep muscles). The efficacy of the proposed FL-based and conventional SMCs is demonstrated via computer simulation within MATLAB/Simulink programming platform. The numerical simulation has been conducted within MALTAB environment using Simulink library blocks which are interacted with written m-functions. The mathematical model and control algorithm have been developed and coded inside MATLAB m-functions. The FL-based SMC Simulink model is illustrated in Figure 3. Parameters' setting is given in Table 4.

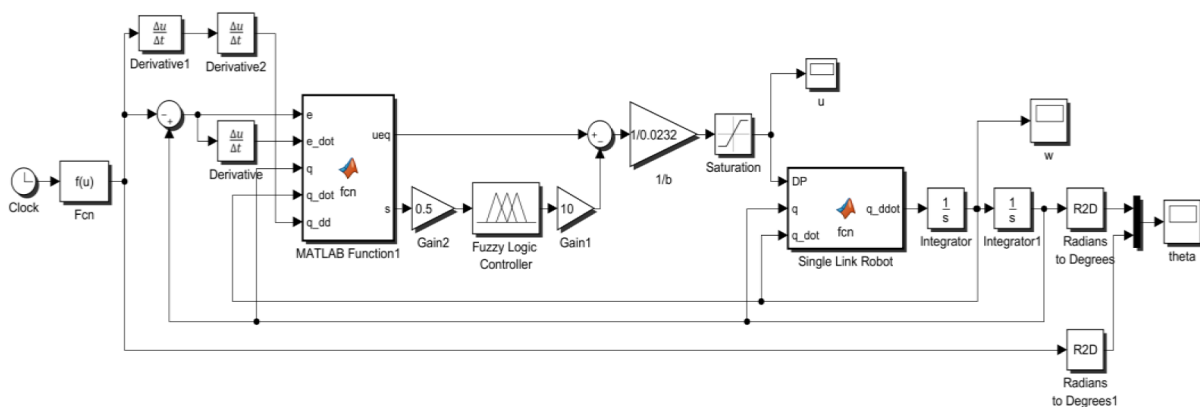


FIGURE 3. Simulink modelling of FL-based SMC

The desired angular position  $\theta_d$  is suggested from the well-known literature equation [12]:

$$\theta_d = \frac{\pi}{2} + 0.5 (\sin(2\pi f_1 t) + \sin(2\pi f_2 t) + \sin(2\pi f_3 t))$$

where  $f_1 = 0.02$  Hz,  $f_2 = 0.05$  Hz and  $f_3 = 0.09$  Hz are the proposed frequencies for such function. Figure 4 shows the behaviors of desired and actual angular positions of

TABLE 4. Physical system parameters [12]

Description of system parameter	Value	Unit
Force applied by the PAM $F_0$ (Nominal)	0.986	N
The change in force applied by PAM $F_1$	0.803	N
Coefficient of bicep viscosity $B_{0b}$ (Nominal)	1.35	N·s/m
The deviation in bicep viscosity coefficient $B_{1b}$	$4.66 \times 10^{-3}$	N·s/m
Tricep viscosity coefficient $B_{0t}$ (Nominal)	0.403	N·s/m
The variation tricep viscosity coefficient $B_{1t}$	$12 \times 10^{-4}$	N·s/m
Spring coefficient $k_0$ (Nominal)	6.51	N/m
Link mass $M$	20	Kg
Devaition in spring coefficient $k_1$	$2.12 \times 10^{-2}$	N/m
Radius of pulley $r$	$5.08 \times 10^{-2}$	m
Gravitational acceleration $g$	9.81	m/s <sup>2</sup>
Bicep pressure $P_{0b}$ (Nominal)	$0.510 \times 10^3$	K·Pa
Tricep pressure $P_{0t}$ (Nominal)	$4 \times 10^2$	K·Pa
Distance $L$	0.46	m
Distance $a$	$7.02 \times 10^{-2}$	m

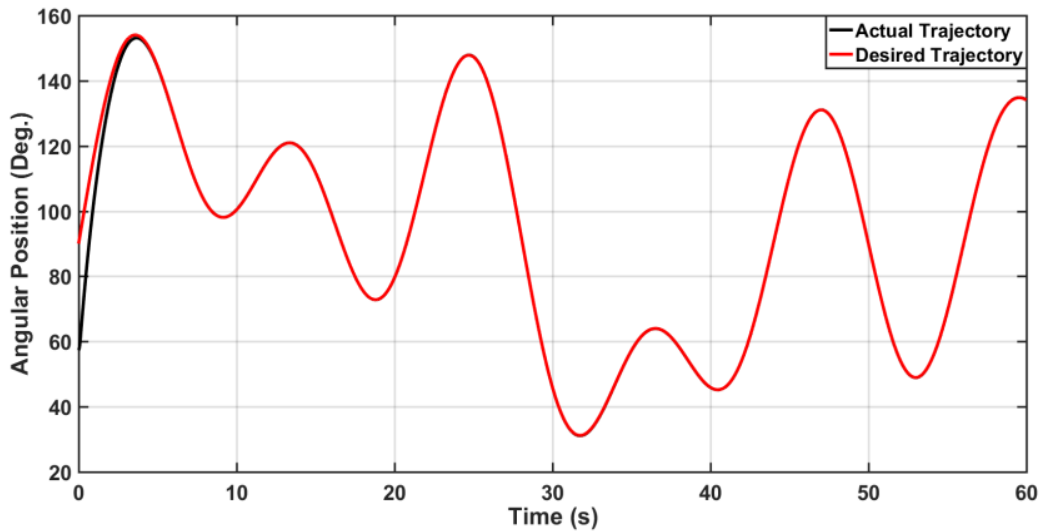


FIGURE 4. (color online) The behaviors of desired and actual angular positions of robot link in case of Signum-based SMC

robot link in case of classical SMC. It is clear that the conventional SMC could give good tracking performance and there is negligible error between the desired and actual angular positions of the robot link. Figure 5 shows the angular velocity of the robot link. Figure 6 shows the control signal actuating the robot link. This actuating signal represents the amount of pressure has to be applied to the muscles to achieve the required angular position. It is evident from the figure that there is high chattering in control signals which may lead to defectives in used PAM actuators. In addition, the conventional SMC absorbs high control efforts as the pressure source have to supply maximum pressure at specified times of control task.

In Figure 7, the desired and actual angular positions are demonstrated in case of incorporating the fuzzy logic block to synthesize the control law of actuating signal. The figure shows that there is no complete coincidence of both desired and actual trajectories.

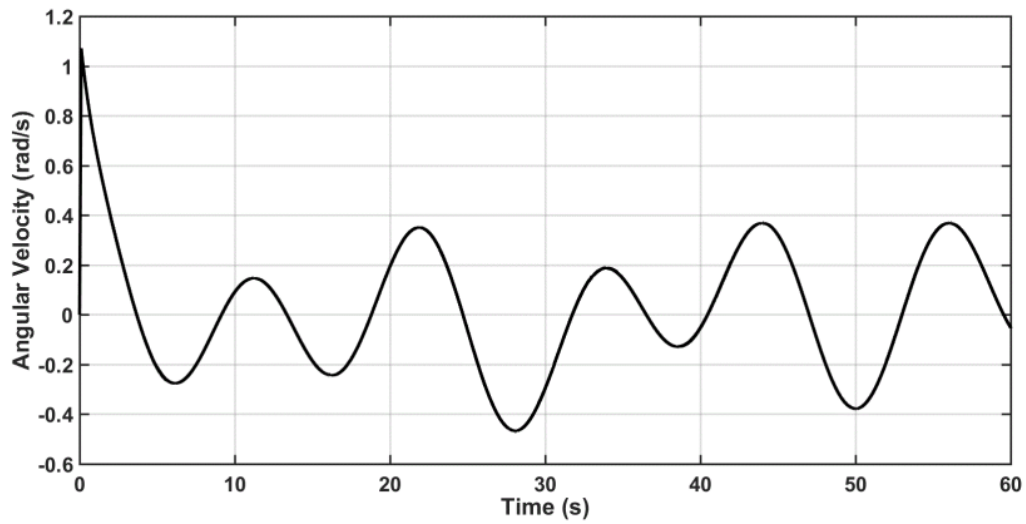


FIGURE 5. The behavior angular velocity of robot link

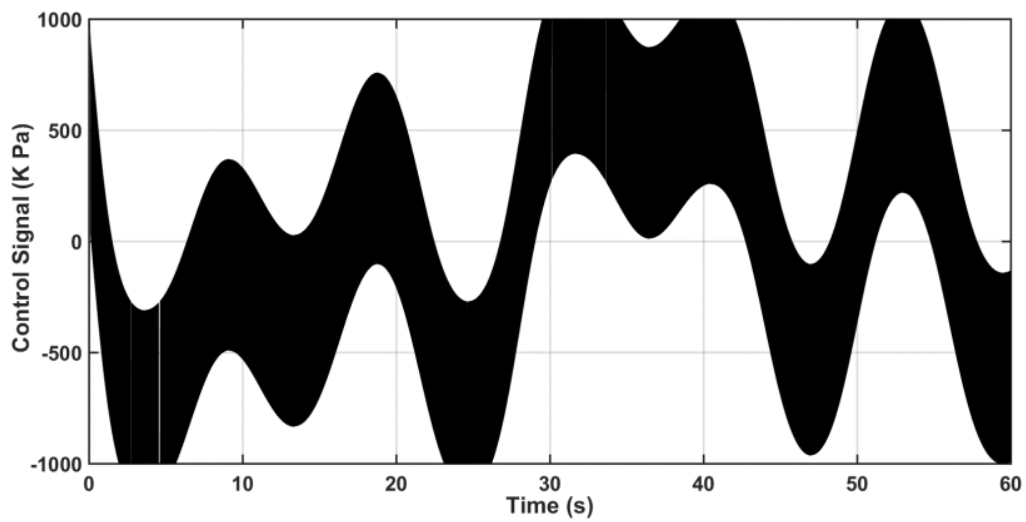


FIGURE 6. The behavior control signal in case of Signum-based SMC

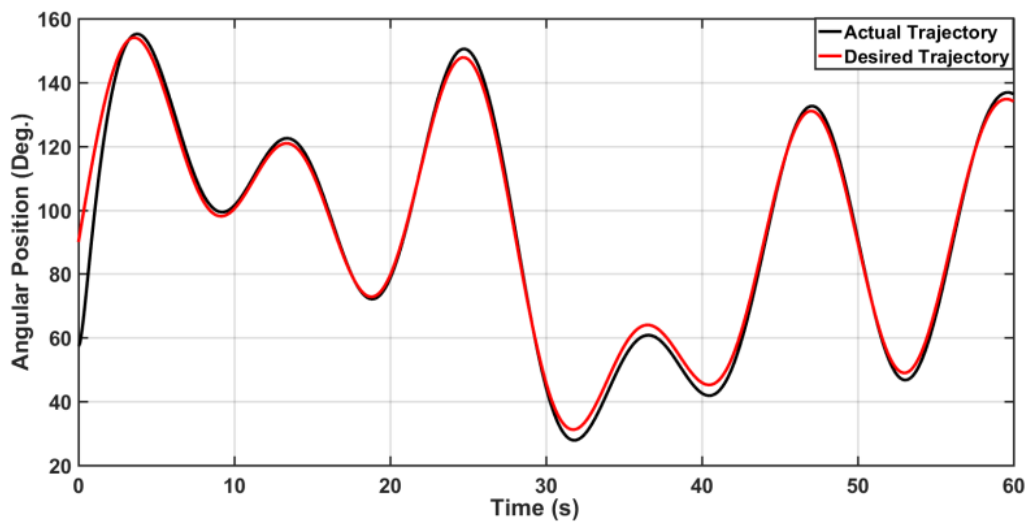


FIGURE 7. (color online) The behaviors of desired and actual angular positions of robot link in case of FL-based SMC

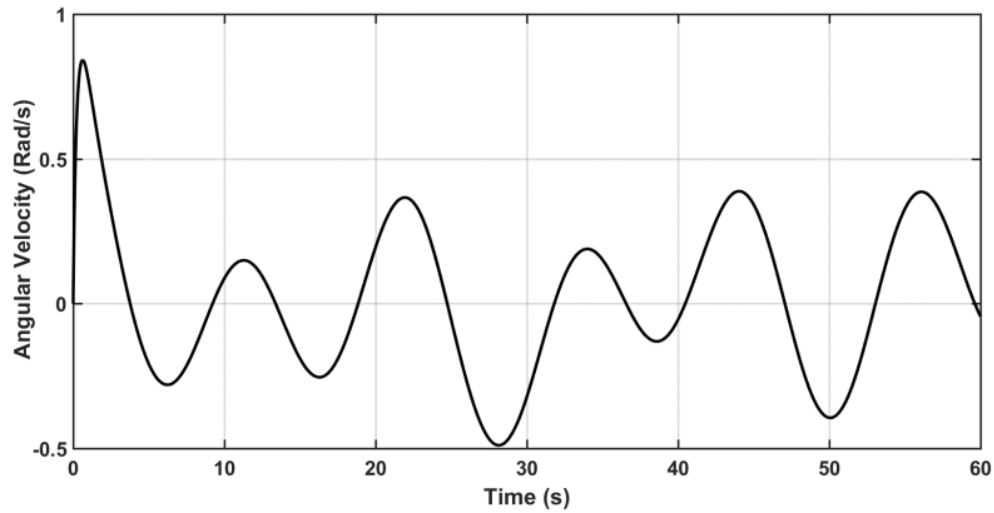


FIGURE 8. The behavior angular velocity of robot link

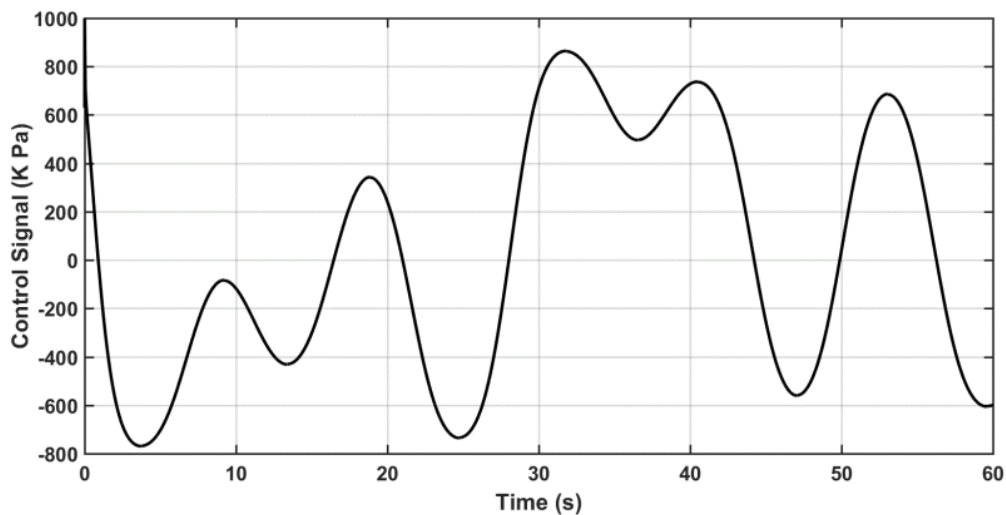


FIGURE 9. The behavior control signal in case of FL-based SMC

However, tuning of membership functions may lead to zero tracking error, which is beyond the scope of this study. Figure 8 shows the behavior of angular velocity for robot link.

On the other side, the chattering which has been shown in conventional SMC has disappeared in the control signal as illustrated by Figure 9. In addition, the control signal did not exceed the prescribed limits of pressurized source. This in turn led to lower cost of exhaustive pressure to be absorbed by the controlled system as compared to higher cost in the previous SMC. However, the price to be paid by this improvement in the chattering behavior is the degradation in tracking performance.

**6. Conclusions.** In this study, the Signum function used as switching part in the control law of SMC has been synthesized by FL system. The proposed FL system objective is the chattering reduction due to applying the Signum function in the feedback control law. Firstly, the design of SMC based on Signum function is developed to control angular position of PAM-actuated single-link manipulator. A comparison study between FL-based SMC and Signum-based SMC has been conducted in terms of chattering and dynamic performance. The numerical simulation showed that the chattering due to Signum function has been considerably reduced when using FL system to replace the hard switching function. However, introducing the FL system could degrade the tracking performance

of controlled robot unless parameters of FL system have to be tuned. These parameters include number and shape of MFs, knowledge base information, input and output gains of FL system. One can suggest future work by using different optimization methods to tune these design parameters for further reduction of chattering effect [39-45].

#### REFERENCES

- [1] M.-S. Chen and M.-L. Tseng, A new design for noise-induced chattering reduction in sliding mode control, in *Sliding Mode Control*, InTech, DOI: 10.5772/15507, 2011.
- [2] H. Lee, *Chattering Suppression in Sliding Mode Control System*, Ph.D. Thesis, The Ohio State University, 2007.
- [3] K. J. Kim, J. B. Park and Y. H. Choi, Chattering free sliding mode control, *SICE-ICASE International Joint Conference 2006*, Bexco, Busan, Korea, 2006.
- [4] A. F. Mutlak and A. J. Humaidi, A comparative study of synergetic and sliding mode controllers for pendulum systems, *Journal Européen des Systèmes Automatisés*, vol.56, no.5, pp.871-877, <https://doi.org/10.18280/jesa.560518>, 2023.
- [5] J. J. E. Slotine and W. Li, *Applied Nonlinear Control*, Prentice Hall Englewood Cliffs, NJ, 1991.
- [6] Y. Yang, Y. Wang, W. Zhang, Z. Li and R. Liang, Design of adaptive fuzzy sliding-mode control for high-performance islanded inverter in micro-grid, *Energies*, vol.15, no.23, 9154, 2022.
- [7] M.-L. Tseng and M.-S. Chen, Chattering reduction of sliding mode control by low-pass filtering the control signal, *Asian Journal of Control*, vol.12, no.3, pp.392-398, 2010.
- [8] A. Sahamijoo, F. Piltan, M. H. Mazloom, M. R. Avazpour, H. Ghiasi and N. B. Sulaiman, Methodologies of chattering attenuation in sliding mode controller, *International Journal of Hybrid Information Technology*, vol.9, no.2, pp.11-36, 2016.
- [9] N. Cibiraj and M. Varatharajan, Chattering reduction in sliding mode control of quad-copters using neural networks, *Energy Procedia*, vol.117, pp.885-892, 2017.
- [10] A. J. Humaidi and A. F. Hasan, Particle swarm optimization-based adaptive super-twisting sliding mode control design for 2-degree-of-freedom helicopter, *Measurement and Control (United Kingdom)*, vol.52, nos.9-10, pp.1403-1419, 2019.
- [11] Y. Yang and Y. Yan, Attitude regulation for unmanned quadrotors using adaptive fuzzy gain-scheduling sliding mode control, *Aerospace Science and Technology*, vol.54, pp.208-217, 2016.
- [12] J. H. Lilly and L. Yang, Sliding mode tracking for pneumatic muscle actuators in opposing pair configuration, *IEEE Transactions on Control Systems Technology*, vol.13, no.4, pp.550-558, 2005.
- [13] N. Tsagarakis and D. G. Caldwell, Improved modeling and assessment of pneumatic muscle actuators, *Proc. of the IEEE International Conference on Robotics and Automation*, San Francisco, CA, USA, vol.4, pp.3641-3646, 2000.
- [14] D. G. Caldwell, G. A. Medrano-Cerda and M. J. Goodwin, Braided pneumatic actuator control of a multi-jointed manipulator, *Proc. of the IEEE Systems Man and Cybernetics Conference (SMC)*, vol.1, pp.423-428, 1993.
- [15] A. J. Humaidi, I. K. Ibraheem, A. T. Azar and M. E. Sadiq, A new adaptive synergetic control design for single link robot arm actuated by pneumatic muscles, *Entropy*, vol.22, 723, 2020.
- [16] T. Choi, J. Lee and J. Lee, Control of artificial pneumatic muscle for robot application, *2006 IEEE/RSJ International Conference on Intelligent Robots and Systems*, pp.4896-4901, 2006.
- [17] A. K. Al Mhdawi, N. Wright, A. J. Humaidi and A. T. Azar, Adaptive PI-fuzzy like control of a stack pneumatic actuators testbed for multi-configuration small scale soft robotics, *2023 International Conference on Manipulation, Automation and Robotics at Small Scales (MARSS)*, Abu Dhabi, United Arab Emirates, pp.1-8, DOI: 10.1109/MARSS58567.2023.10294122, 2023.
- [18] S. William, H. Oswaldo and M. S. H. Tsuzuki, Pneumatic artificial muscle optimal control with simulated annealing, *IFAC-PapersOnLine*, vol.51, no.27, pp.333-338, 2018.
- [19] K. Tarapong and P. Radom, Adaptive control for a one-link robot arm actuated by pneumatic muscles, *Chiang Mai Journal of Science*, vol.35, no.3, pp.437-446, 2008.
- [20] J. H. Lilly, Adaptive tracking for pneumatic muscle actuators in bicep and tricep configurations, *IEEE Transactions on Neural Systems and Rehabilitation Engineering*, vol.11, no.3, pp.333-339, 2003.
- [21] S. Boudoua, M. Hamerlain and F. Hamerlain, Intelligent twisting sliding mode controller using neural network for pneumatic artificial muscles robot arm, *2015 International Workshop on Recent Advances in Sliding Modes (RASM)*, pp.1-6, 2015.
- [22] D. G. Caldwell, G. A. Medrano-Cerda and M. Goodwin, Control of pneumatic muscle actuators, *IEEE Control Systems Magazine*, vol.15, no.1, pp.40-48, 1995.

- [23] A. Falah, A. J. Humaidi, A. Al-Dujaili and I. K. Ibraheem, Robust super-twisting sliding control of PAM actuated manipulator based on perturbation observer, *Cogent Engineering*, vol.7, no.1, 1858393, 2021.
- [24] A. J. Humaidi and A. H. Hameed, PMLSM position control based on continuous projection adaptive sliding mode controller, *Systems Science & Control Engineering*, vol.6, no.3, pp.242-252, DOI: 10.1080/21642583.2018.1547887, 2018.
- [25] A. J. Humaidi, S. Hasan and A. A. Al-Jodah, Design of second order sliding mode for glucose regulation systems with disturbance, *International Journal of Engineering and Technology*, vol.7, no.2, pp.243-247, 2018.
- [26] J. Guo, Y. Liu, J. Zhou and G. Wang, A new nonlinear sliding mode control system design, *The 27th Chinese Control and Decision Conference (2015 CCDC)*, pp.4490-4493, 2015.
- [27] A. Q. Al-Dujaili, A. Falah, A. J. Humaidi, D. A. Pereira and I. K. Ibraheem, Optimal super-twisting sliding mode control design of robot manipulator: Design and comparison study, *International Journal of Advanced Robotic Systems*, vol.17, no.6, 2020.
- [28] A. H. Hameed, A. Q. Al-Dujaili, A. J. Humaidi and H. A. Hussein, Design of terminal sliding position control for electronic throttle valve system: A performance comparative study, *International Review of Automatic Control*, vol.12, no.5, pp.251-260, 2019.
- [29] N. S. Mahmood, A. J. Humaidi, R. S. Al-Azzawi and A. Al-Jodah, Extended state observer design for uncertainty estimation in electronic throttle valve system, *International Review of Applied Sciences and Engineering*, vol.15, no.1, pp.107-115, <https://doi.org/10.1556/1848.2023.00662>, 2024.
- [30] Z. A. Waheed and A. J. Humaidi, Design of optimal sliding mode control of elbow wearable exoskeleton system based on whale optimization algorithm, *Journal Européen des Systèmes Automatisés*, vol.55, no.4, pp.459-466, 2022.
- [31] Z. A. Waheed, A. J. Humaidi, M. E. Sadiq, A. A. Al-Qassar, A. F. Hasan, A. Q. Al-Dujaili, A. R. Ajel and S. J. Abbas, Control of elbow rehabilitation system based on optimal-tuned backstepping sliding mode controller, *Journal of Engineering Science and Technology*, vol.18, no.1, pp.584-603, 2023.
- [32] S. S. Husain, M. Q. Kadhim, A. S. M. Al-Obaidi, A. F. Hasan, A. J. Humaidi and D. N. Al-Husaeni, Design of robust control for vehicle steer-by-wire system, *Indonesian Journal of Science and Technology*, vol.8, no.2, pp.197-216, 2023.
- [33] H. Y. Abed, A. T. Humod and A. J. Humaidi, Type 1 versus type 2 fuzzy logic speed controllers for brushless DC motors, *International Journal of Electrical and Computer Engineering*, vol.10, no.1, pp.265-274, 2020.
- [34] A. F. Ghaleb, A. A. Oglah, A. J. Humaidi, A. S. M. Al-Obaidi and I. K. Ibraheem, Optimum of fractional order fuzzy logic controller with several evolutionary optimization algorithms for inverted pendulum, *International Review of Applied Sciences and Engineering*, vol.14, no.1, pp.1-12, <https://doi.org/10.1556/1848.2021.00375>, 2023.
- [35] T. Ghanim, A. R. Ajel and A. J. Humaidi, Optimal fuzzy logic control for temperature control based on social spider optimization, *IOP Conference Series: Materials Science and Engineering*, vol.745, no.1, 012099, 2020.
- [36] N. M. Noaman and O. A. Mohammad, Adaptive hybrid neural fuzzy controller using augmented error method, *Proc. of the 2006 IEEE GCC Conference (GCC)*, Manama, Bahrain, pp.1-5, 2006.
- [37] A. J. Humaidi, H. T. Najem, A. Q. Al-Dujaili, D. A. Pereira, K. I. Ibraheem and A. T. Azar, Social spider optimization algorithm for tuning parameters in PD-like interval Type-2 fuzzy logic controller applied to a parallel robot, *Measurement and Control*, vol.54, nos.3-4, pp.303-323, 2021.
- [38] A. R. Nasser, A. T. Azar, A. J. Humaidi, A. K. Al-Mhdawi and I. K. Ibraheem, Intelligent fault detection and identification approach for analog electronic circuits based on fuzzy logic classifier, *Electronics*, vol.10, no.23, 2888, 2021.
- [39] M. Y. Hassan, A. J. Humaidi and M. K. Hamza, On the design of backstepping controller for Acrobot system based on adaptive observer, *International Review of Electrical Engineering*, vol.15, no.4, pp.328-335, <https://doi.org/10.15866/iree.v15i4.17827>, 2020.
- [40] M. N. Noaman, A. S. Gatea, A. J. Humaidi, S. K. Kadhim and A. F. Hasan, Optimal tuning of PID-controlled magnetic bearing system for tracking control of pump impeller in artificial heart, *Journal Européen des Systèmes Automatisés*, vol.56, no.1, pp.21-27, 2023.
- [41] N. Q. Yousif, A. F. Hasan, A. H. Shallal, A. J. Humaidi and L. T. Rasheed, Performance improvement of nonlinear differentiator based on optimization algorithms, *Journal of Engineering Science and Technology*, vol.18, no.3, pp.1696-1712, 2023.
- [42] R. S. Al-Azzawi and M. A. Simaan, On the selection of leader in Stackelberg games with parameter uncertainty, *International Journal of Systems Science*, vol.52, no.1, pp.86-94, 2021.

- [43] M. N. Ajaweed, M. T. Muhssin, A. J. Humaidi and A. H. Abdulrasool, Submarine control system using sliding mode controller with optimization algorithm, *Indonesian Journal of Electrical Engineering and Computer Science*, vol.29, no.2, pp.742-752, 2023.
- [44] R. S. Al-Azzawi and M. A. Simaan, Sampled closed-loop control in multi-controller multi-objective control systems, *SoutheastCon 2018*, Petersburg, FL, USA, pp.1-7, 2018.
- [45] R. S. Al-Azzawi and M. A. Simaan, Leader-follower controls in systems with two controllers, *2019 SoutheastCon*, Huntsville, USA, pp.1-6, 2019.